Program Digest, 2019 IEEE International Ultrasonics Symposium (IUS)
Glasgow, Scotland, October 6-9, 2019

Simulation of Standing Wave Reduction in HIFU Transcranial Tumors Therapy

1st Yanqiu Zhang
Tianjin Medical University
Biomedical Engineering
Tianjin, China
15620610782@126.com

2st Hao Zhang
Tianjin Medical University
Biomedical Engineering
Tianjin, China
15222659805@163.com

3st Ting Pan
Tianjin Medical University
Biomedical Engineering
Tianjin, China
13163095669@163.com

4st Xiqi Jian
Tianjin Medical University
Biomedical Engineering
Tianjin, China
jianxiqi@tmu.edu.cn

***Abstract*—When the High Intensity Focused Ultrasound phase-controlled transducer is used for transcranial treatment of brain tumors, the continuous therapeutic ultrasound emitted by the phase-controlled transducer and the reflected wave at the high-acoustic impedance skull can easily form a standing wave.This results in loss of energy and possible damage to normal tissue.In this study, a numerical simulation model was built using 82-element phase-controlled transducers and volunteer skull CT data. According to the conditions of breaking the standing wave formation, the method of intracranial and standing wave reduction was studied by numerical simulation method, which provided a basis for the clinical safety, technical methods and theoretical data of brain tumors.**

Keywords—standing wave, High Intensity Focused Ultrasound , simulation, transcranial

I. INTRODUCTION

High Intensity Focused Ultrasound (HIFU) utilizes the tissue penetration and focusability of ultrasound [1] to focus the tissue-free, low-intensity ultrasound emitted by the extracorporeal transducer in the body to be treated [2]. Under the action of the biological effects of ultrasound, the treatment of coagulation necrosis in the body to be treated to a temperature above 54 °C [3]. However, due to the large difference in acoustic characteristics between the skull and the surrounding soft tissue, when the HIFU phase-controlled transducer is treated by brain tumor, the continuous therapeutic ultrasound emitted by the transducer meets the reflected wave at the high acoustic impedance skull to form a standing wave, resulting in loss of energy and possibly causing damage to normal tissue. In this study, we can reduce the standing wave by breaking the standing wave formation condition, improve the transcranial focusing performance of the phase-controlled transducer, and prevent the damage of normal tissues, and provide treatment methods and data for safe and effective transcranial treatment.

II. METHODS

A. Westervelt acoustic wave nonlinear propagation equation

The acoustic nonlinear propagation equation expression is as follows [4]:

$$\nabla^2 p-\frac{1}{c^2}\frac{\partial^2 p}{\partial t^2}+\frac{\delta}{c^4}\frac{\partial^3 p}{\partial t^3}+\frac{\beta}{\rho c^4}\frac{\partial^2 p^2}{\partial t^2}=0 \quad (1)$$

In this equation, ∇ is the Laplace operator, p (Pa) is the acoustic pressure, t(s) is time, ρ (kg/m3) and c (m/s) are density and sound velocity of the acoustic medium respectively, δ is the acoustic diffusion coefficient and $\delta=\frac{2c_0^3\alpha}{\omega^2}$ where α (dB/mm) is the acoustic attenuation coefficient, β is the nonlinear coefficient, $\omega=2\pi f$ (rad/s) is angular frequency and f is the drive frequency of the transducer.

B. Standing wave reduction methodthe

Under the condition that the frequency of the therapeutic ultrasonic wave is kept constant, the sinusoidal signal is used as the basic excitation signal, the Randi function is used to generate the 0, π random phase, and the generated random phase is added to the basic excitation signal at regular time intervals to break the standing wave formation condition. The excitation signal of the array element i is:

$$S_{ipa}(\mathrm{t})=I_i\sin(\omega(\mathrm{t}+\Delta \mathrm{t}_i)+\varphi(t)) \quad (2)$$

Where φ is phase shift which from a random sequence of 0 or π (produced by a random function). It is invoked when $t=nT_r$ (n=1, 2, 3…) in which T_r is the time segment of random phase transformation, and frequency of phase transformation is $f_r=\frac{1}{T_r}$. $R_a=\frac{P_{\max}-P_{\min}}{P_{avg}}$ is standing-wave ratio which used to value the intensity of standing waves, P_{max} is the peak amplitude, P_{min} is the minimum amplitude, P_{avg} is the average amplitude of the region. R_a are increasing with the intensity of standing waves.

C. Numerical simulation model and parameters

As shown in Fig. 1, a numerical simulation model of HIFU transcranial treatment was established by combining the head CT data of 58-year-old healthy female volunteers (provided by Tianjin Medical University Cancer Hospital) with the 82-element semi-randomly distributed spherical crown phase transducer (radius 80 mm, opening diameter 100 mm).

Project supported by the National Natural Science Foundation of China (81272495) and the Natural Science Foundation of Tianjin (16JC2DJC32200)

Wherein, the phase-controlled transducer selects the center position of each array element under the condition that the spacing of adjacent array elements is not less than 1.0 mm, and the radius of the array element is 4 mm. The spatial step size of the numerical simulation is $dx = dy = dz = 0.25$mm, and the time step of the numerical simulation is $dt = 10$ns. The model boundary is processed by the Mur first-order boundary absorption condition.

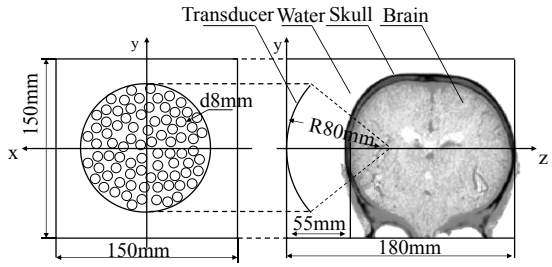

Fig. 1. Numerical simulation model of HIFU trancranial treatment.

In this study, the parameters of the skull and brain tissue such as , c, were obtained based on the high resolution CT. This study was approved by the ethics committee of Tianjin Medical University, Tianjin, China, and written informed consent was obtained from the volunteer. The slice thickness and spacing were both 3 mm. The parameters were obtained from bone porosity (Φ) converted from the Hounsfield unit (H) of the CT images and the calculation method was as follow [5,6]:

$$\Phi = 1 - \frac{H}{1000} \tag{3}$$

$$\rho = \Phi \times \rho_{\text{water}} + (1-\Phi) \times \rho_{\text{bone}} \tag{4}$$

$$c = c_{\text{water}} + (1-\Phi) \times (c_{\text{bone}} - c_{\text{water}}) \tag{5}$$

$$\alpha = \alpha_{water} + (\Phi)^{0.5} \times (\alpha_{bone} - \alpha_{water}) \tag{6}$$

Here ρ_{bone} , c_{bone} , α_{bone} and are density, speed of sound and attenuation of cortical skull bone respectively ρ_{water} , c_{water} , α_{water} are density, speed of sound and attenuation of water respectively. Other parameters used in the simulation [7,8] are shown in table 1.

TABLE I. CONSTANT PARAMETERS USED IN THE SIMULATION

	ρ (kg/m^3)	c (m/s)	α (dB/m)	r_{ec} (W·m^{-1}·K)	C_B (J·kg^{-1}·K)
Water	998	1486	0.2	4180	0.6
Cortical skull	1600	3200	8	1840	1.3

III. RESULTS AND DISCUSSION

A. Results

Fig. 2 shows the sound pressure field formed by numerical simulation without standing wave reduction. The white curve shows the skull, and the red arrow shows the standing wave generated by the intracranial and extracranial. Fig. 3(a)(b) shows the focal point of the time segment T_r and the maximum sound pressure at the bone and its bone coke ratio. It can be seen from Fig. 3 that the sound pressure at the focus and the maximum sound pressure at the bone increase after the standing wave is reduced. In addition, bone coke ratio shows a concussively decreasing trend. Fig. 4 shows the variation of the standing wave ratio with the time segment T_r. As can be seen from Fig. 4, when the T_r is the same, the intracranial R_a is larger than the extracranial R_a. As T_r increases, the entire area R_a, extracranial R_a, and intracranial R_a gradually increase. Figure 5 (a)(b) is the sound pressure field before and after standing wave is reduced, and (c) is the corresponding sound pressure curve. As can be seen from Figure 5, after the standing wave is reduced, the sound pressure at the focus and the sound pressure at the skull are increase.At the same time, The sound pressure curve is more stable and the fluctuation is concussively reduced.

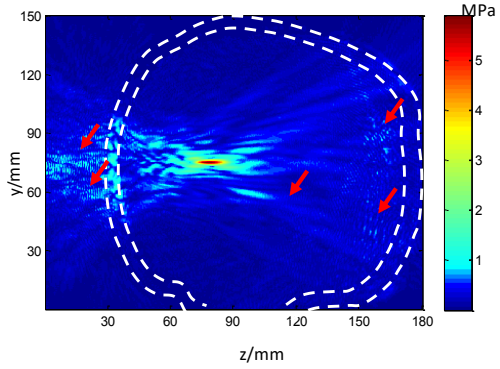

Fig. 2. Numerical simulation model of HIFU trancranial treatment.

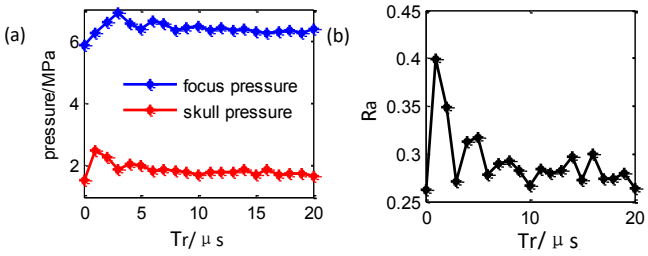

Fig. 3. The sound pressure field, (a) maximum pressure with segment time, (b) skull and focus ratio

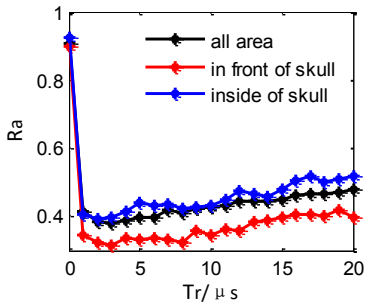

Fig. 4. Standing wave ratio with conversion cycle

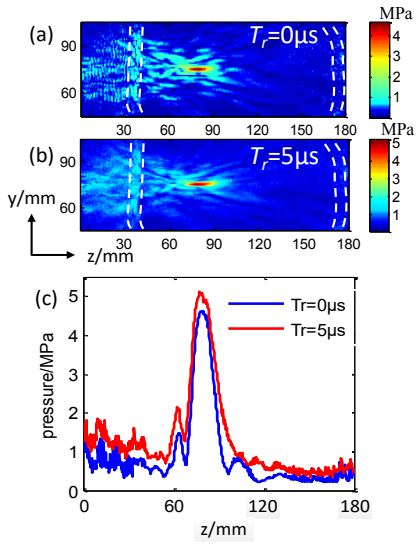

Fig. 5. The sound pressure field is compared, (a) (b) is the sound pressure field before and after the standing wave is reduced, and (c) is the sound pressure curve.

Fig.6 is the variation curve of the focal position offset distance with the T_r. It can be seen from Fig.6 that the focus shift of the focus in the negative direction of the z-axis is more obvious after the standing wave is reduced, that is, the focus moves closer to the side of the transducer. Fig. 7 is a graph showing the area of the focal field within the sound pressure field half-sound pressure point -6 dB and its long and short axis as a function of the conversion period Tr. It can be seen from Fig. 7 that the area of the focal region after the standing wave is reduced, the length of the long axis, and the length of the short axis are increased.

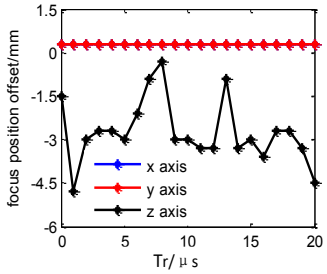

Fig. 6. The focus position offset distance with T_r.

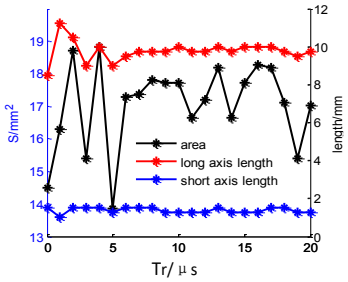

Fig. 7. The area of the focal length, long and short axis with T_r.

B. Discussion

In this study, only one volunteer's skull CT information was used for modeling and simulation. For different patients, the skull structure parameters are different, which may affect the standing wave. In order to analyze the influence of the radius of curvature and thickness of the skull on the formation of standing waves, The internal and external surface coordinates (x_{in}, y_{in}, z_{in}) and (x_{out}, y_{out}, z_{out}) of the skull are used to calculate the thickness distribution of the skull in the acoustic window,

$$\mathrm{d}(x_{out}, y_{out}) = \min\left(\sqrt{(x_{out}-x_{in})^2+(y_{out}-y_{in})^2+(z_{out}-z_{in})^2}\right) \quad (7)$$

Calculating the mean distance of each point on the outer surface of the skull from the position of the center of the sphere as the geometric radius of the outer surface of the skull in the acoustic window,

$$Rc = \sqrt{x^2+y^2+(z-z_c)^2} \quad (8)$$

Z_c is to set the bone acoustic window to the spherical center coordinate of the approximate sphere. Figure 8 shows the numerical simulation model of the HIFU transsacral treatment established by taking the average cranial bone density, sound velocity and attenuation coefficient from the real skull parameters of the volunteers, forming Fig.9 and Fig.10 (R_c=75.5mm) and Fig.11 and Fig.12 (d=5.1mm) show the sound pressure field distribution map and the corresponding standing wave ratio curve.

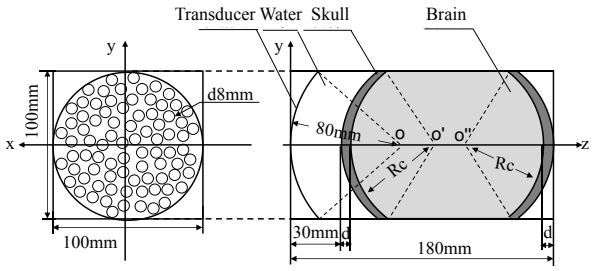

Fig. 8. numerical simulation ideal model of HIFU trancranial treatment.

It can be seen from Fig. 9 to Fig. 12 that the standing wave ratio is affected by the thickness and curvature of the skull and may cause secondary focusing, which may cause damage to normal tissues.

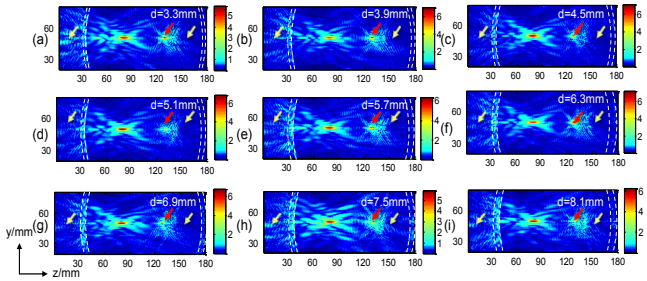

Fig. 9. Sound pressure field formed by different thickness. (R_c=73.5mm)

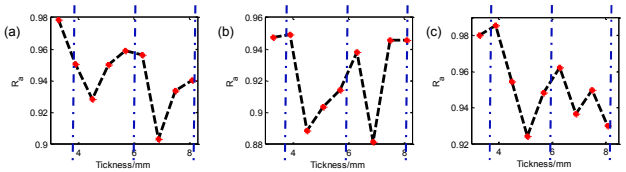

Fig. 10. Standing wave ratio with thickness curve. (a) extracranial, (b) intracranial, (c) full area.

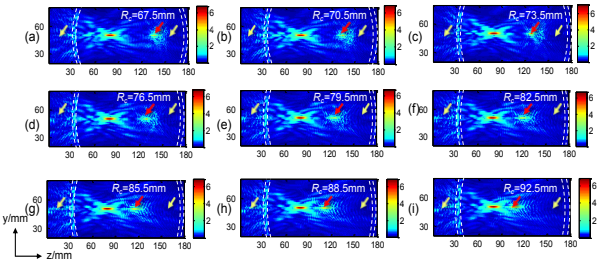

Fig. 11. Sound pressure field formed by different thickness. (d=5.1mm)

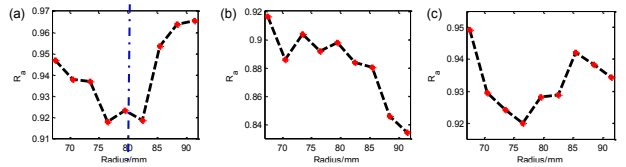

Fig. 12. Standing wave ratio with curvature curve. (a) extracranial, (b) intracranial, (c) full area.

IV. Conclution

In this paper, the random phase breaking standing wave generation condition is added to the excitation signal of the phase-controlled transducer to realize the standing wave reduction. The numerical simulation results show that the method can effectively reduce the standing wave. Through explore the ideal skull numerical simulation model, show that Skull thickness and curvature have an effect on the generation of standing waves. Statistical analysis of multi-person head CT modeling is under investigation.

References

[1] Wood R, Loomis A. The physical and biological effects of high-frequency sound-waves of great intensity[J]. Philos Mag Ser, 1927, 4 (22): 417-436.

[2] Lynn J, Putnam T. Histology of cerebral lesions produced by focused ultrasound[J]. The American journal of pathology, 1944, 20(3): 637.

[3] Fry W, Mosberg W ,Barnard J , et al. Production of focal destructive lesions in the central nervous system with ultrasound[J]. Neurosurg , 1954 .11:471-478.

[4] Pernot M, Aubry J F, Tanter M, et al. High power transcranial beam steering for ultrasonic brain therapy[J]. Physics in medicine and biology, 2003, 48(16): 2577-2589.

[5] Leduc N, Okita K, Sugiyama K, et al. Focus Control in HIFU Therapy Assisted by Time-Reversal Simulation with an Iterative Procedure for Hot Spot Elimination[J]. Journal of Biomechanical Science & Engineering, 2012, 7(1):43-56.

[6] Ding X, Wang Y, Zhang Q, et al. Modulation of transcranial focusing thermal deposition in nonlinear HIFU brain surgery by numerical simulation.[J]. Physics in Medicine & Biology, 2015, 60(10):3975.

[7] Thomas J, Fink M. Ultrasonic beam focusing through tissue inhomogeneities with a time reversal mirror: application to transskull therapy[J]. IEEE Transactions on Ultrasonics Ferroelectrics and Frequency Control, 1996, 43(6):1122 - 1129.

[8] Tang S, Clement G. Standing-Wave Suppression for Transcranial Ultrasound by Random Modulation[J]. IEEE Transactions on Biomedical Engineering, 2010, 57(1):203-205.